



Compaction and bending variability measurements of a novel geometry 3D woven layer to layer interlock composite textile around a 90° curve plate 3.2 mm radius



Spiridon Koutsonas

Ulster University/NIACE (North Ireland Advanced Composites Engineering Centre), Faculty Computing and Engineering/NIACE Advanced Composites and Engineering, Belfast, N.I., UK

ARTICLE INFO

Keywords:

Composites
Textile
Compaction
Variability
90° bend 3.2 mm radius curve plate

ABSTRACT

The aim of this investigation is to measure compaction and bending variability of a novel composite 3D woven textile layer-to-layer interlock around a 90° curve plate geometry. To that, end with the use of an empirical power law the compaction behaviour of the novel weave geometry textile fitted. This way it is possible to evaluate the max shear stress at 90° during bending. The preform thickness variation along the bending was measured with the use of a Coordinate Measurement Machine. The overall methodology and data variability measurements are useful for the manufacturing process of composites at macro-scale level as predictive data in Resin Transfer Moulding flow analysis for a complex composite node with 90° bend moulder geometry.

1. Introduction

Compaction behaviour inside the mould cavity and corresponding V_f determines the local fabric permeability and so is directly related to race-tracking and preform variability. In order to address preform compaction a number of models by Chen et al. [1] have been proposed.

Robitaille and Gauvin [2–4] published studies of the compaction of textile reinforcements for composites manufacturing. The power law Eq. (1), has been used as the base for unsaturated and saturated empirical compaction models by Govignon et al. [5] in simulation of the reinforcement compaction and resin flow during the complete resin transferred moulding infusion process, and also by Bickerton and Buntain [6], Correia [7], Endruweit and Long [8], Summerscales and Searle [9].

$$V_f = \alpha_c P^\beta \quad (1)$$

In Eq. (1) V_f is the fibre volume fraction, P is the pressure, α_c and β are empirical material constants. The Eq. (1) implies that the fibre volume fraction is zero when the pressure is zero the equation may work if a limited range of V_f are considered. A more appropriate model is given by Toll and Manson [10] for elastic compression of a disperse planer fiber network

$$P = \frac{512}{5\pi^4} E f^4 (V_f - V_{f0}) \quad (2)$$

Where P is the applied pressure, E is the young's modulus of the fiber

orientation distribution as defined by Toll, V_f is the fiber volume fraction, f^4 is an empirical carbon fiber material characteristic. The second term V_{f0} is a parameter that needs adjustment but tends to be negligible at realistic fibre volume fractions. So if V_{f0} is zero when the pressure is zero the Eq. (2) will become (2.1)

$$P = \frac{512}{5\pi^4} E f^4 V_f \quad (2.1)$$

and so with organization of the V_f against the Pressure will be the (2.2)

$$V_f = \frac{1}{E f^4} P^{\frac{5\pi^4}{512}} \quad (2.2)$$

which becomes the Eq. (1).

2. Methodology and materials

Composite processing and modelling requires effective materials characterisation. Testing environments need to be representative of the manufacturing method since the results will be used in simulation tools. In this way, it is necessary to understand the main factors affecting the material property and design a test routine that considers these factors. Compaction characterisation for this study was conducted in a similar fashion by Correia [7]. A purpose built machined test rig, (see Fig. 1a) consisted of a matched top moving part and a lower fixed 50 mm internal diameter circular fitting, which were fixed to a dual-column, Instron 5969 tester. For consistency and reflect to previous findings on

E-mail address: s.koutsonas@ulster.ac.uk.

<http://dx.doi.org/10.1016/j.coco.2017.06.004>

Received 18 May 2017; Received in revised form 12 June 2017; Accepted 21 June 2017
2452-2139/ Crown Copyright © 2017 Published by Elsevier Ltd. All rights reserved.

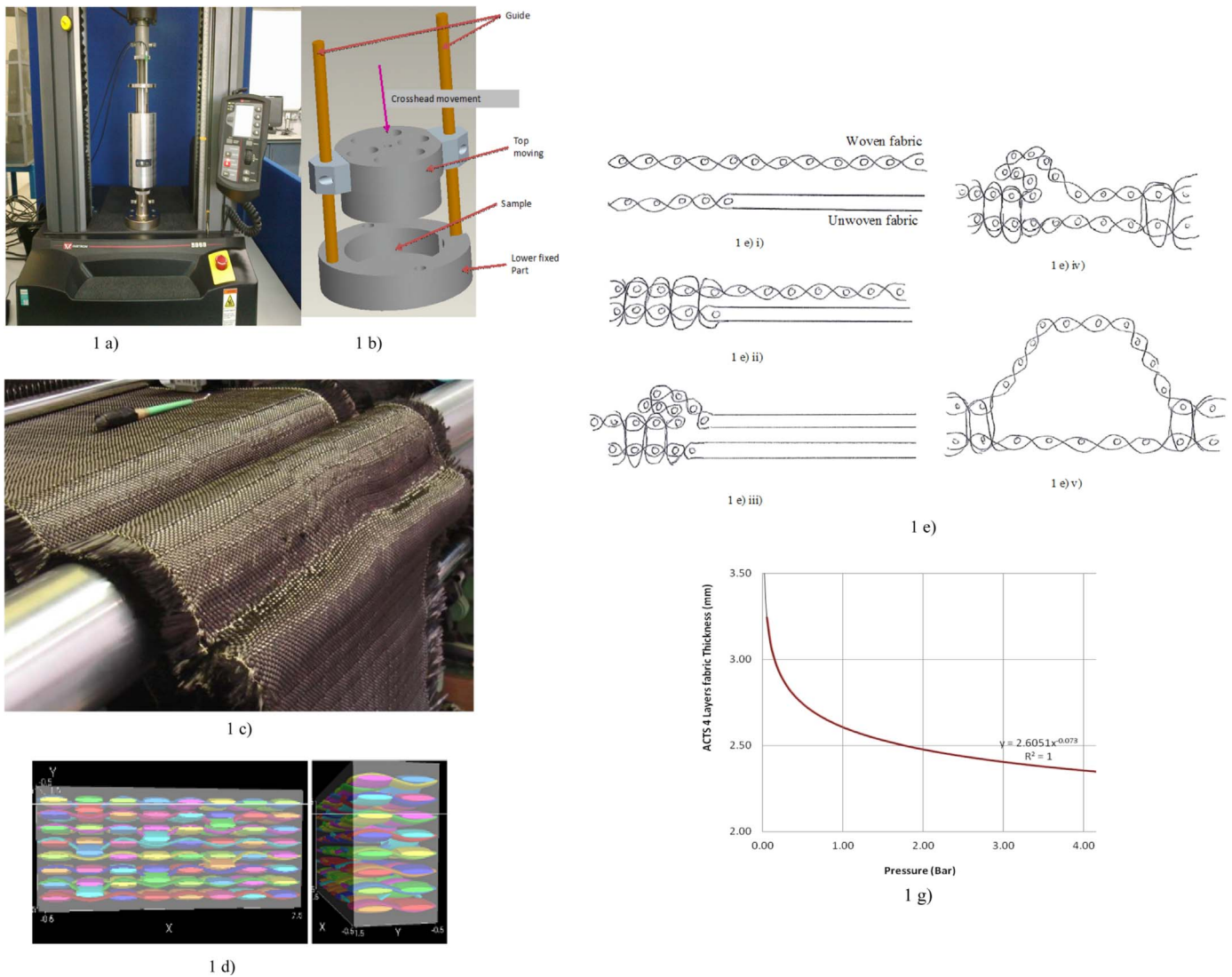


Fig. 1. a) Instron 5969 model compaction testing rig, 1 b) Schematic of fabric compression test, 1 c) Reinforcement used for compaction tests 3D woven made off HTS40 F13, 1 d): Design of the Sigmatex textile used for textile used for compaction and bending measurements. Image generated using Tex-Gen software. X-axis coincides with the weft direction and Y-axis coincide with the warp direction of the fabric, 1 e) i) Shows a fabric which is woven and a fabric which is unwoven, 1 e) ii) Shows a fabric which has 2 layers with the upper portion woven and lower portion unwoven, 1 e) iii) Shows the bound fabric where the upper portion is folded over to form a loop during the weaving process, 1 e) iv) Shows how the material appears after weaving has recommenced with the upper portion longer in length than the lower portion 1 e) v) Shows how the structure could be formed to create a defined cross Section, 1 g) Compaction and fitting equation of the 3D woven layer to layer interlock textile.

layer effects, reinforcement samples were press-cut into 50 mm discs and loaded into the lower fixed plate sample fitting cavity, see Fig. 1a). Dry samples of the novel architecture 3D woven fabric were compacted at a rate of 1 kN/s, from zero to 10 kN static load capacity. An aut-ranging load cell used to measure force as shows Fig. 1b).

To enable the determination of absolute distance (specimen height H) between the upper moving plate and the lower fixed plate cavity of the rig during testing, a linear displacement transducer was used in order to calculate the fibre volume fraction at each state of compression according to Eq. (3) Endruweit [8].

$$V_f = \frac{m}{\rho AH} \tag{3}$$

where m is the specimen mass, A is the specimen area, and ρ is the density of the carbon fibres. The Eq. (3) is an adaptation of the more complete Eq. (3.1) in CRAG method 1000 for the measurement of the engineering properties of fibre reinforced plastics, royal aerospace establishment technical report 88012, February 1988 as presented by Curtis [11].

$$V_f = \frac{nA_F}{\rho H} \tag{3.1}$$

Where n is the number of layers, A_F the aerial weight of the fabric, ρ is the density of the carbon fibres, H the thickness of the laminate.

With the combination of (1) and (3):

$$H_{fabricthickness} = \alpha P^{-\beta} \tag{4}$$

In Eq. (4) the preform thickness H is related to a given compaction pressure P , where $\alpha = \frac{m}{\rho A \alpha_c}$ and β are empirical material constants. The instrumentation and materials tested presented in Fig. 1 the material properties in Table 1a) and b).

3D woven HTS40 F13 (Fig. 1c) made from carbon fibres known as Toxo Tenax® HTS40 F13. These are commercial high strength aerospace grade carbon fibres 12k for yarn in warp, weft and binder as shows Fig. 1d). The textile is one layer composed of eight weft yarns with measured thickness of (5.85 ± 0.05) mm made of HTS40 F13 carbon fibres with carbon fibres density $\rho = 1760 \text{ kg/m}^3$. The aerial mass was calculated as the ratio of mass density, m , over surface area, A , and it

Table 1

a): Textiles with properties used in compaction tests, b): Compaction tests power law fitting according to Eq. (3), (c): Measured h_{min} thickness of 3D woven for HTS40 F13 fabric in warp, (d): Measured h_{min} thickness of 3D woven for HTS40 F13 fabric in weft direction.

1 a)			
Textile type	Textile commercial name	Manufacturer	Aerial mass (kg/m ²)
3D- woven	HTS40 F13	Sigmatex Ltd	2.284 (4-layers)

1 b)		
Preform	Layers	H height (mm)
3D- woven angle interlock fabric	4-layers	$2.6051P^{(-0.073)}$

was found to be: 5.30 kg/m². The fibre volume fraction calculated from Eq. (2). The 3D interlock weave used on this research is woven in multiple layers and the multiple layers are woven such that a loop is formed in the fabric. The loop of the structure is such that the distance between the upper fabric surface and lower fabric surface is different. The woven structure has areas that have all layers joined and areas that are not joined which are then able to form loops.

During the standard weaving process, the fabric is drawn away from the loom by a set of rollers. This process is continuous and the fabric that is produced is of a defined length. The preferred embodiment of

this invention is to weave a structure where one surface is woven with at least 2 threads in both warp and weft directions and the other surface consists of 2 different areas, one woven with interlacing threads and one which consists of both woven and unwoven threads. When the fabric which is woven forming the longer surface is at the required length, the woven material is advanced to the point where the other unwoven section begins. The unwoven section is then re-woven. The weaving of all layers continues from the point where both areas of woven fabric ends to form a continuous fabric with a loop.

There are many applications requiring structural rigidity where this type of material can be used as a stiffener and where an angle is required in a 3D structure. By controlling the shape of the loop during subsequent processing with resin infusion moulding, further structural integrity can be achieved.

3D woven fabric properties and measured thickness around 90° bend presented on Appendix A Table 1a).

3. Compaction results and discussion

After HTS40 F13 preform characterisation was completed the results of compaction tests data collected to a PC, to which the Instron 5969 model tester was connected. The empirical power law then fitted and the pressure (bar) against fabric thickness (mm) plotted 4-layers. The results presented on Appendix A Table 1c), d) (nesting considered negligible due to binder of 3D woven geometry).

Nesting of plies was not considered as previous studies by Robitaille, and Gauvin [2–4], Govignon et al. [5], Bickerton, et al. [6] had

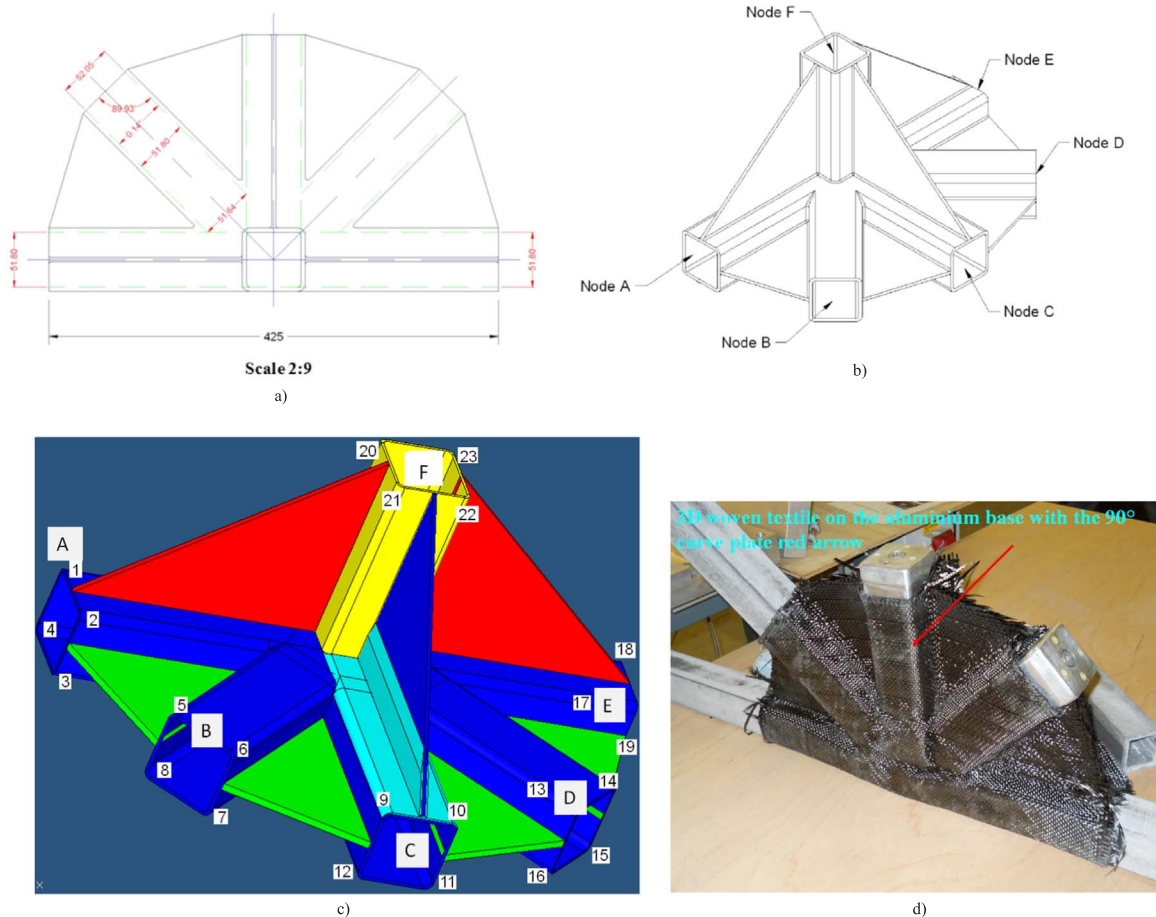


Fig. 2. a) CAD design of ACTS aluminium metallic insert generic node length in mm upper view, 2 b) ACTS generic node strut members A to F, 2 c) CAD node model with the assigned struct twenty-three 90° zones, 2 d) CMM test on the aluminium insert rectangular base with 90° curve plates used as zero (reference) firstly for the data acquisition probe and secondly with the 3D woven textile, red arrow shows the 90° curve plate extracted from the random number generator for CMM measurements. (For interpretation of the references to color in this figure legend, the reader is referred to the web version of this article.)

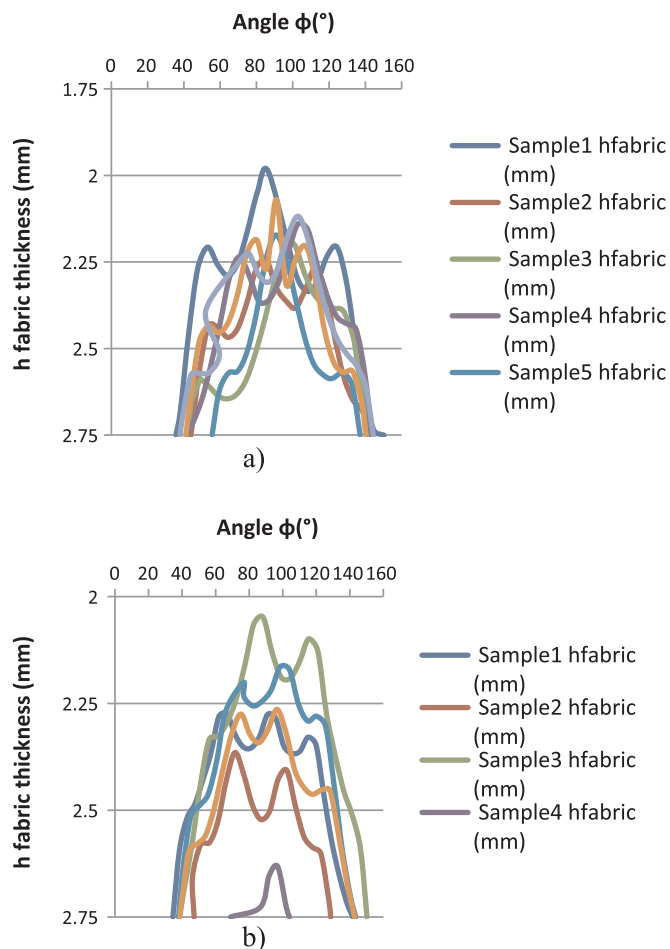


Fig. 3. a): Measured fabric thickness variation on bending with HTS40 F13 3D woven samples warp 4-layers preform, 3 b): Measured fabric thickness variation on bending with HTS40 F13 3D woven samples weft 4-layers preform.

suggested this to be negligible, for two neighbouring layers of the same plain woven fabric. This way, it is possible to evaluate the preform thickness at any pressure value i.e. max shear stress at 90° during bending.

4. Bending

When a fibrous preform bends around a radius it is compacted radially at the bend part due to in-plane tension caused by friction between the compacted preform and the tool as discussed by Dong [12]. In order to measure the bending behaviour the aluminium moulder insert 3D base with a 90° curved plate and 3.2mm radius designed and constructed as shows Fig. 2.

5. Coordinate measuring machine tests

A coordinate measuring machine (CMM) Mitutoyo Crysta-Apex S model s900 is a 3D device for measuring the physical geometrical characteristics of an object. The above CCM machine has a guaranteed resolution of 0.0001 mm according the specifications of the manufacturer [13]. MPP-300Q Scanning Probe ultra-high-accuracy and performance multi-function Mitutoyo probe used for the measurements. The internal scales provide a resolution of 0.01 μm in all axes and air bearings guarantee best directionality. Measuring force is so low (a minimum of 0.03 N) that even elastic work-pieces such as resins, etc., can be measured without damage or distortion. An MPP-300Q Scanning probe attached to the third moving axis of this machine defines measurements. The CAT 1000S freeform surface evaluation program

installed on a desktop which was connected with the CMM machine was used for the surface topology of the fabric. The probe was firstly scanned the aluminium base node without the fabric and created a reference CAD file. Secondly the aluminium node scanned again with the 3D woven interlock fabric and a second CAD file was generated. The distance of the two CAD files gave the CCM measurements of the novel geometry 3D woven layer to layer interlock composite textile around a 90° curve plate 3.2 mm radius as shows Fig. 3a) and b).

6. Procedure

With the use of the above-mentioned instrumentation, the bending behaviour of the textile in Table 1 was tested. Firstly, the node divided to struck members A, B, C, D, E, F secondly to each one of the generic node struck shown in Fig. 2c), d), a sub group of 90° zones was assigned as follows: node member A - (zones 1, 2, 3, 4), node member B - (zones 5, 6, 7, 8), node member C - (zones 9, 10, 11, 12), node member D - (zones 13, 14, 15, 16), node member E - (zones 17, 18, 19) and node member F - (20, 21, 22, 23) thereafter with the use of a random number generator (Appendix B) randomly a 90° zone number indicated and subsequently scanned with CMM. On this case the struck member node C top right lower part was extracted as shows red arrow Fig. 2c) and measured with CMM. In order to define the 3D coordinate system of reference and after 5 samples in warp and 5 samples in weft of the novel 3D woven textile measured at the same reference position.

All measurements conduct with the 3D woven textile mentioned in Fig. 1a)-d) (4-layers ACTS fabric). The output data file collected on a PC to which the CMM machine was connected.

6.1. CMM results

Bending tests results are presented in following Fig. 3(a) to (b) where the gap between the fabric and the upper mould h_{gap} is plotted against the angle ϕ along the curved plate bend.

7. CMM results discussion

Preform thickness measured variations Fig. 3a) – b) were used to generate tables with h_{min} fabric thickness on the 90° bend with approximation up to ± 0.1 mm (show in Appendix A Table 11c)–A d)).

All data compaction variability was collected for use subsequently on a 90° bend moulder thickness of 2.75 mm. So if preform thickness inside mould is 2.75mm on the bend angle was measured to be lower in all tested fabrics. Therefore, the h_{min} fabric thickness on bend Appendix A Table 1c)–A d) revealed the gap height (h_{gap}) variation on the bend.

Preform measured fabric thickness variability on bend presented in Fig. 3a)–b) Section 6.1 may be considered for fitting with a model in order to predict the gap height and so racetrack and variability with simulations flow modelling on RTM process.

In this investigation:

- The compaction behaviour of a novel 3D woven textile was measured and fitted with an empirical law
- Bending variability measurements around a 90° curve plate geometry 3.2 mm radius was effectuated
- Generated tables with h_{min} thickness on the 90° bend from the samples of the tested preform.
- These data may be used for the manufacturing process of a generic node RTM process with the composite textile geometry.

8. Conclusion

CMM experimental contact technique used in order to investigate the compaction and bending variability behaviour of a novel 3D woven composite textile around a 90° curve plate 3.2 mm radius on a 2.75 mm of moulder thickness. CMM data analysis may be used for generating a

model that describes the bending around a 90° curve plate and so as input to simulations of resin flow for analysis of race-tracking variability and void formation that may arise during the manufacturing process of RTM with the composite node presented in Fig. 2.

Acknowledgement

The work reported in this article was carried out under the Innovate

UK collaborative research through Advanced Composites Truss Structures (ACTS) project with industrial partners Airbus, Bentley Motors Ltd, Composites Integration Ltd, Network Rail, NP-Aerospace, Pipex, QinetiQ, Tony Gee, Sigmatex, Oxford Brooks University, and The University of Nottingham. Sincere thanks are extended to my supervisor of this project, Prof. Andrew Long. JEC Composites award was given for the manufacture of the 3D woven preform by Sigmatex, which studied on the analysis presented in this article as part of ACTS project.

Appendix A

CMM measured 3D woven fabric properties and measured thickness around 90° bend. All CMM experimental results with the tested fabric are presented as shown in Table 1(c)-A(d).

1 c)

Sample Num.	h_{\min} fabric thickness on bend(mm)
Sample 1	2
Sample 2	2.2
Sample 3	2.2
Sample 4	2.1
Sample 5	2.2
Sample 6	2.1
Sample 7	2.1

1 d)

Sample Num.	h_{\min} fabric thickness on bend(mm)
Sample 1	2.3
Sample 2	2.4
Sample 3	2
Sample 4	2.6
Sample 5	2.2
Sample 6	2.3

Appendix B

Random numbers generator (C-prog.).

```
#include < stdio.h > .
#include < stdlib.h > .
#include < math.h > .
int GetRand(int min, int max);
int main(void).
{.
int i, rgap;.
for (i = 0; i < 23; i + ).
{.
rgap = GetRand(1,7);
printf ("Gap case %d/n", rgap);.
}.
return(0);.
}.
int GetRand(int min, int max).
{.
static int Init = 0;.
int rgap;.
if (Init == 0).
{.
/*
* As Init is static, it will remember it's value between.
* function calls. We only want srand() run once, so this.
* is a simple way to ensure that happens.
```

```

*/.
srand(time(NULL));
Init = 1;
}.
/*
* Formula:
* rand() % N < - To get a number between 0 - N-1.
* Then add the result to min, giving you.
* a random number between min - max.
*/.
rgapc = (rand() % (max - min + 1) + min);
return (rgapc);
}.

```

References

- [1] B. Chen, E.J. Lang, T.-W. Chou, Experimental and theoretical studies of fabric compaction behavior in resin transfer molding, *Mater. Sci. Eng.: A* 317 (2001) 188–196.
- [2] F. Robitaille, R. Gauvin, Compaction of textile reinforcements for composites manufacturing. I: review of experimental results, *Polym. Compos.* 19 (2) (1998) 198–216.
- [3] F. Robitaille, R. Gauvin, Compaction of textile reinforcements for composites manufacturing. II: compaction and relaxation of dry and H₂O-saturated woven reinforcements, *Polym. Compos.* 19 (5) (1998) 543–557.
- [4] F. Robitaille, R. Gauvin, Compaction of textile reinforcements for composites manufacturing. III. Reorganization of the fiber network, *Polym. Compos.* 20 (1) (1999) 48–61.
- [5] Q. Govignon, S. Bickerton, P.A. Kelly, Simulation of the reinforcement compaction and resin flow during the complete resin infusion process, *Compos. Part A—Appl. Sci. Manuf.* 41 (1) (2010) 45–57.
- [6] S. Bickerton, M.J. Buntain, Modeling forces generated within rigid liquid composite molding tools. Part B: numerical analysis, *Compos. Part A—Appl. Sci. Manuf.* 38 (7) (2007) 1742–1754.
- [7] N. Correia, Thesis “Analysis of the vacuum infusion moulding process” University of Nottingham, School of Mechanics Materials, Manufacturing Engineering and Management Chapter 3: (April 2004); p 40–73.
- [8] A. Endruweit, A.C. Long, Analysis of compressibility and permeability of selected 3d woven reinforcements, *J. Compos. Mater.* 44 (24) (2010) 2833–2862.
- [9] J. Summerscales and T.J. Searle Low-pressure (vacuum infusion) techniques for moulding large composite structures, *J. Materials: Design and Applications*, Proceedings IMechE Vol. 219 Part L: p. 45–58 <http://dx.doi.org/10.1243/146442005X10238>.
- [10] S. Toll, J.A.E. Manson, Elastic compression of a fiber network, *J. Appl. Mech.* 62 (1) (1995) 223–226, <http://dx.doi.org/10.1115/1.2895906>.
- [11] P.T. Curtis. CRAG test methods for the measurements of the engineering properties of fibre reinforced plastics, Royal Aerospace Establishment, Technical Report 88012, February 1988.
- [12] C. Dong, Model development for the formation of resin-rich zones in composites processing, *Composites: Part A* 42 (2011) 419–424.
- [13] http://www.mitutoyo.com/wp-content/uploads/2013/01/2097_CRYSTA_ApexS.pdf, Last assessed 12.06.2017.